Magnetic properties and martensitic transition in annealed $Ni_{50}Mn_{30}Al_{20}$

Lluís Mañosa[a] and Antoni Planes
Facultat de Física, Universitat de Barcelona, Diagonal, 647, E-08028 Barcelona, Catalonia, Spain

Mehmet Acet, Eyup Duman, and Eberhard F. Wassermann
Tieftemperaturphysik, Gerhard-Mercator Universität Duisburg, D-47048 Duisburg, Germany

(Presented on 15 November 2002)

We have studied the effect of heat treatment on the magnetic properties and on the martensitic transition of the $Ni_{50}Mn_{30}Al_{20}$ alloy. A mixed $L2_1+B2$ state is obtained in the as-prepared sample, while no $L2_1$ order is retained in the sample quenched from high temperature. For the two heat treatments, the samples order antiferromagnetically, but there is evidence of coexisting ferromagnetic interactions. A martensitic transition occurs below the magnetic one for quenched samples. However, the martensitic transition is inhibited in the as-prepared sample. © *2003 American Institute of Physics.* [DOI: 10.1063/1.1555977]

Magnetic alloys undergoing structural transitions have received much attention due to the peculiar properties arising from the coupling between structure and magnetism. Among them, magnetic field induced strains[1] and magnetocaloric effect[2] are of particular interest due to their potential application as sensors and actuators and as magnetic refrigerators. This article reports results on Ni–Mn–Al alloys, which are potential candidates to exhibit giant magnetic field induced strains.[3] These magnetic induced strains occur in ferromagnetic systems undergoing a martensitic transformation. They originate from the reorientation of martensite domains promoted by the difference in the Zeeman energy.[4] Currently, the only alloy which has shown giant (up to 10%) deformations[5] is the Ni–Mn–Ga alloy, for compositions close to the stoichiometric Ni_2MnGa. However, the brittleness of this alloy has prompted the research of alternative materials.

It was established[6,7] that for Ni–Mn–Ga, the phase stability is controlled by the average number of valence electrons per atom. In Fig. 1 we compare the phase diagram of Ni–Mn–Al to that of Ni–Mn–Ga. It is assumed that the number of valence electrons per atom for Ni, Mn, Ga, and Al atoms are 10 ($3d^8\,4d^2$), 7 ($3d^5\,4s^2$), 3 ($4s^2\,4p^1$), and 3 ($3s^2\,3p^1$), respectively. The phase diagram of Ni–Mn–Al agrees with the restricted data previously published.[8] From the figure it is clear that for this alloy, the stability of the different phases is controlled by the valence electron concentration as occurs with Ni–Mn–Ga. The phase diagrams of the two alloy systems exhibit a number of general trends. At high temperatures the alloys exhibit a nearest-neighbors ordered structure, B2 ($Pm3m$), and upon cooling, next-nearest neighbors order, $L2_1$ ($Fm3m$) is expected to develop. For Ni–Mn–Al, the transition line for this order–disorder transition is located at temperatures significantly lower than for Ni–Mn–Ga. This results in a very slow kinetics for the ordering process, and recent studies on a stoichiometric compound[9] have shown that long time annealings just below the order–disorder line do not stabilize a single $L2_1$ phase, but rather a mixed $L2_1+B2$ state. This is in contrast to Ni–Mn–Ga alloys for which the B2–$L2_1$ transition occurs very fast.[10] At temperatures close to room temperature, magnetic ordering occurs. The $L2_1$ phase is ferromagnetic and for Ni–Mn–Al, the magnetic ordering in the pure B2 phase is conical antiferromagnetic. The mixed $L2_1+B2$ state incorporates ferromagnetic and antiferromagnetic parts for which close-

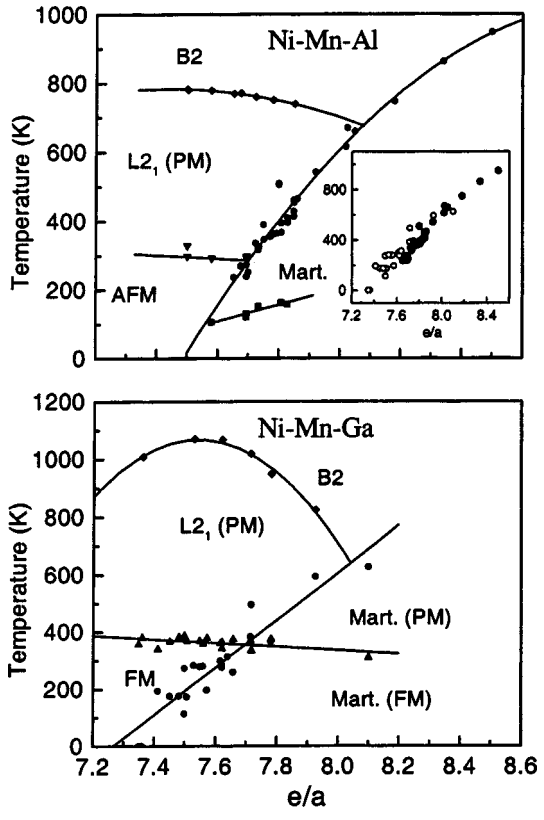

FIG. 1. Phase diagrams of Ni–Mn–Al and Ni–Mn–Ga as a function of the electron concentration. The inset shows data for the martensitic transition temperature for Ni–Mn–Al (solid symbols) and for Ni–Mn–Ga (open symbols). Data are collected from Refs. 6, 8, 10–12, and 16. Lines are guides to the eye.

[a]Electronic mail: lluis@ecm.ub.es

 © 2003 American Institute of Physics

Downloaded 09 Jun 2010 to 161.116.168.169. Redistribution subject to AIP license or copyright; see http://jap.aip.org/jap/copyright.jsp

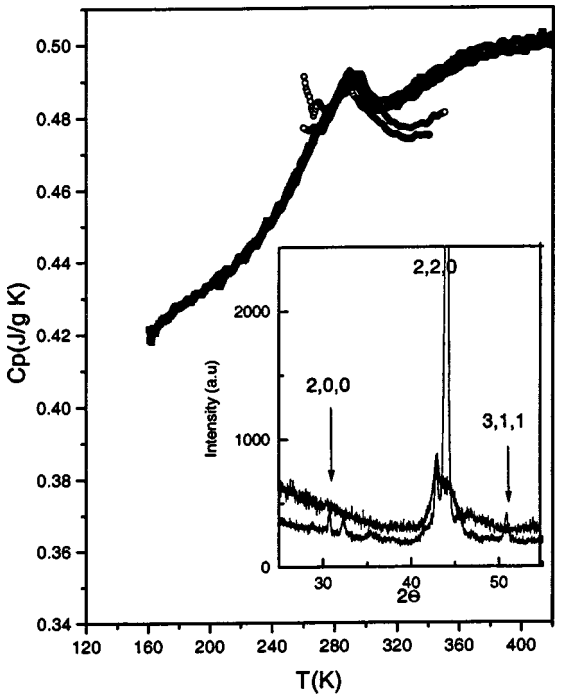

FIG. 2. Specific heat as a function of temperature for as-prepared (solid symbols) and quenched (open symbols) samples. The inset shows the x-ray spectrum for the as-prepared (bottom curve) and quenched (upper curve) samples.

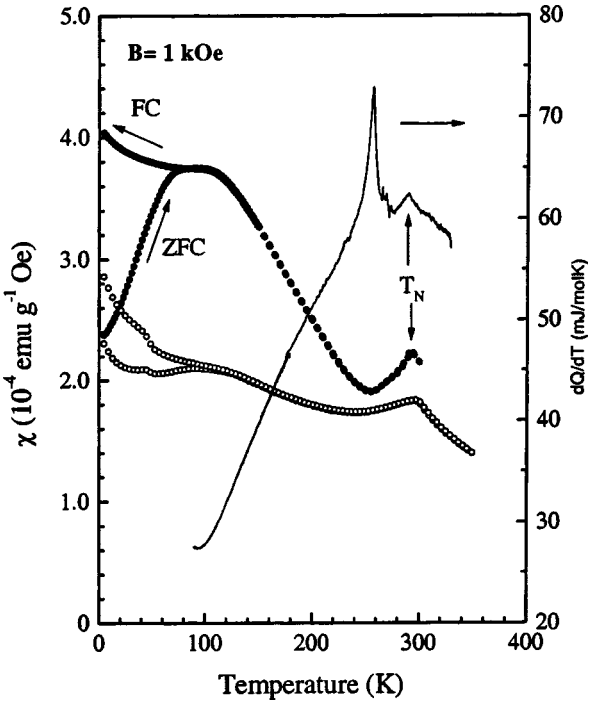

FIG. 3. Temperature dependence of the FC and ZFC magnetic susceptibility for the as-prepared (open symbols) and quenched (solid symbols) samples. Continuous line corresponds to the thermal curve measured for a quenched sample.

lying Curie and Néel temperatures are identified from magnetization measurements.[9] As a consequence of the mixed magnetic interactions in this alloy system there is pinning of the ferromagnetic parts caused by the antiferromagnetic environment, as evidenced by the splitting in the field cooled and zero field cooled magnetic susceptibility measurements. The temperature below which pinning is observed is also shown in Fig. 1 (squares), and has been attributed by some authors to the occurrence of a spin–glass transition.[11] For both alloy systems, the martensitic transition exhibits a marked dependence on the electron concentration. The martensitic transition is mainly accomplished by a shear mechanism, and volume effects are negligible. For this reason, it is expected that the transition temperature will not be very much affected by substitutional effects, provided that the valence electrons are unchanged. Such an assumption is confirmed in the inset of Fig. 1 which shows that the martensitic transition temperatures (M_s) for both Ni–Mn–Al and Ni–Mn–Ga alloys collapse (within experimental errors) on a single line.

The sample studied in this work was prepared by induction melting in an Ar atmosphere in a water cooled Cu crucible. The composition of the sample was determined by EDX analysis to be 50.2 at % Ni, 29.6 at % Mn, and 20.2 at % Al, which is very close to the composition of one of the samples reported in Ref. 12. Samples with typical dimensions $4\times2\times1$ mm^3 were cut from the prepared ingot by using a low speed diamond saw. Two different heat treatments were investigated: slow cooling from the melt (as-prepared sample), and annealing at 1373 K for three days and subsequent quench in water at room temperature (quenched sample). The structure was examined by x-ray diffraction on the polycrystalline samples. Susceptibility measurements were carried out in a field cooled (FC) and zero-field-cooled (ZFC) sequence using a SQUID magnetometer in the temperature range 4 K$\leqslant T\leqslant$400 K and using a vibrating sample magnetometer in the temperature range 300 K$\leqslant$600 K. The specific heat was measured in the interval 150 K$\leqslant T\leqslant$500 K in a modulated differential scanning calorimeter with a temperature modulation of 0.5 K, with a period of 80 s and a heating/cooling rate of 2 K/min. Heat flux (thermal curves) was measured using a nonconventional high sensitivity differential scanning calorimeter, in the temperature range 100 K$\leqslant T\leqslant$320 K.

The specific heat $C_p(T)$ of the samples with the two different heat treatments are shown in Fig. 2. The upturn of the curve for the quenched sample below 270 K is due to the onset of the martensitic transition in that sample. The inset shows the results of the x-ray measurements in the interval $25°\leqslant 2\Theta\leqslant 55°$. The locations of the expected reflection peaks are indicated by the arrows. Because of texturing in the polycrystalline specimens, the relative intensities are not in proportion. The broad character of the peaks for the quenched sample indicates the presence of strains created during the quench. For the as-prepared sample, the emergence of a peak at the position of the (311) reflection indicates the presence of the $L2_1$ phase. For both heat treatments, the specific heat curves exhibit a distinct peak at 289 K for the quenched sample and at 294 K for the as-prepared one. This peak corresponds to the antiferromagnetic transition. For the as-prepared sample the results are similar to those of the stoichiometric sample but quenched stoichiometric samples did not exhibit the antiferromagnetic transition.[13]

Downloaded 09 Jun 2010 to 161.116.168.169. Redistribution subject to AIP license or copyright; see http://jap.aip.org/jap/copyright.jsp

The temperature dependence of the magnetic susceptibility $\chi(T)$ of the two samples is shown in Fig. 3. $\chi(T)$ in FC and ZFC states exhibits a peak at 293 K for the quenched sample and at 297 K for the as-prepared one. These values are somewhat higher than the temperature of the peak in the specific heat. For the studied sample $e/a=7.70$ and the antiferromagnetic transition temperature falls well on the magnetic transition line shown in Fig. 1. It is worth mentioning that quenched stoichiometric samples did not exhibit such a peak, consistent with $C_p(T)$ measurements. A salient feature in Fig. 3 is the splitting between the FC and the ZFC data. Such a splitting that occurs below a magnetic transition is usually an indication of different configurational pinning of residual or intrinsic ferromagnetic parts by the antiferromagnetic environment. Figure 3 also shows the calorimetric curve (heat flux) measured for the quenched sample. A small peak is observed at the antiferromagnetic transition. The large peak arises from the latent heat released during the martensitic transition. For the actual composition, the martensitic structure is expected to be 10M $(5R)$.[12] No traces of the martensitic transition have been detected for the as-prepared sample. Some authors[12] associated the small calorimetric peaks above the martensitic transition with the development of a premartensitic structure. Figure 3 shows that this peak arises from the magnetic transition.

The integration of the calorimetric curve enables to determine the latent heat and the entropy change at the martensitic transition. The obtained values are $\Delta H \simeq 38$ J/mol and $\Delta S \simeq 0.15$ J/mol K. These values are unusually low when compared to the values reported for Ni–Mn–Ga alloys ($\Delta H \simeq 100$ J/mol and $\Delta S \simeq 0.5$ J/mol K) transforming to the same martensitic structure.[14,15] It is expected that different alloy systems undergoing a martensitic transition between the same crystallographic phases exhibit similar values for the entropy change.[16] The low values found here may indicate that only a portion of the sample is actually transforming to martensite.

To conclude, it has been shown that in Ni–Mn–Al, the stability of the different phases is controlled by the electron to atom ratio. The differences in the magnetic behavior of Ni–Mn–Al and Ni–Mn–Ga arise from the slow ordering kinetics in Ni–Mn–Al, due to the low values of the atomic ordering temperatures. For Ni–Mn–Al, the magnetic state contains both ferromagnetic and antiferromagnetic interactions. The martensitic transition has been found to be very sensitive to the degree of atomic order; no transition occurs in the mixed $L2_1+B2$ state. Further investigation is being done, aimed at establishing the exact conditions for the occurrence of the martensitic transition.

This work has received financial support from the CICyT (Spain), MAT2001-3251, and the CIRIT (Catalonia), Project No. 2001SGR00066. M.A. also acknowledges financial support provided by IBERDROLA.

[1] K. Ullakko, J. K. Huang, C. Kantner, R. C. O'Handley, and V. V. Kokorin, Appl. Phys. Lett. **69**, 1966 (1996).
[2] V. K. Pecharsky and K. A. Gschneider, Jr., Phys. Rev. Lett. **78**, 4494 (1997); O. Tegus, E. Brüch, K. H. J. Buschow, and F. R. de Boer, Nature (London) **415**, 450 (2002).
[3] A. Fujita, K. Fukamichi, F. Gejima, R. Kainuma, and K. Ishida, Appl. Phys. Lett. **77**, 3054 (2000).
[4] R. C. O'Handley, J. Appl. Phys. **83**, 3263 (1998).
[5] A. Sozinov, A. A. Likhachev, N. Lanska, and K. Ullakko, Appl. Phys. Lett. **80**, 1746 (2002).
[6] V. A. Chernenko, Scr. Mater. **40**, 523 (1999).
[7] X. Jin, M. Marioni, D. Bono, S. M. Allen, R. C. O'Handley, and T. Y. Hsu, J. Appl. Phys. **91**, 8222 (2002).
[8] F. Gejima, Y. Sutou, R. Kainuma, and K. Ishida, Metall. Mater. Trans. A **30**, 2721 (1999).
[9] M. Acet, E. Duman, E. F. Wassermann, Ll. Mañosa, and A. Planes, J. Appl. Phys. **92**, 3867 (2002).
[10] R. W. Overholser, M. Wuttig, and D. A. Neuman, Scr. Mater. **40**, 1985 (1999).
[11] S. Morito, T. Kakeshita, K. Hirata, and K. Otsuka, Acta Mater. **46**, 5377 (1996).
[12] R. Kainuma, H. Nakano, and K. Ishida, Metall. Mater. Trans. A **27**, 4153 (1996).
[13] Ll. Mañosa, A. Planes, Ch. Somsen, Ch. Fell, and M. Acet, J. Phys. IV **11**, Pr8-245 (2001).
[14] V. A. Chernenko, E. Cesari, V. V. Kokorin, and I. N. Vitenko, Scr. Metall. Mater. **33**, 1239 (1995).
[15] A. Planes, E. Obradó, A. Gonzàlez-Comas, and Ll. Mañosa, Phys. Rev. Lett. **79**, 3926 (1997).
[16] A. Planes and Ll. Mañosa, Solid State Phys. **55**, 159 (2001).

Downloaded 09 Jun 2010 to 161.116.168.169. Redistribution subject to AIP license or copyright; see http://jap.aip.org/jap/copyright.jsp